

Article

Efficient Planar Hybrid n-Si/PEDOT:PSS Solar Cells with Power Conversion Efficiency up to 13.31% Achieved by Controlling the SiO_x Interlayer

Chenxu Zhang ¹, Yuming Zhang ^{1,*}, Hui Guo ¹, Qubo Jiang ², Peng Dong ¹ and Chunfu Zhang ^{1,*} 

¹ Wide Bandgap Semiconductor Technology Disciplines State Key Laboratory, School of Microelectronics, Xidian University, Xi'an 710071, China; zhangcx8008@163.com (C.Z.); guohui@mail.xidian.edu.cn (H.G.); dongpeng@spic.com.cn (P.D.)

² School of Electronic Engineering and Automation, Guilin University of Electronic Technology, No. 1 Jinji Road, Guilin 541004, China; boblincoln@sina.com

* Correspondence: zhangym@mail.xidian.edu.cn (Y.Z.); cfzhang@xidian.edu.cn (C.Z.)

Received: 25 April 2018; Accepted: 21 May 2018; Published: 30 May 2018



Abstract: In this work, the effects of the SiO_x interface layer grown by exposure in air on the performance of planar hybrid n-Si/poly(3,4-ethylenedioxythiophene):poly(styrenesulfonate) (PEDOT:PSS) solar cells are investigated. Compared to the cell with a hydrogen-terminated Si surface, the cell with an oxygen-terminated Si surface reveals improved characteristics in power conversion efficiency, increased from 10.44% to 13.31%. By introducing the SiO_x, the wettability of the Si surface can be improved, allowing an effective spread of the PEDOT:PSS solution and thus a good contact between the PEDOT:PSS film and Si. More importantly, it can change the polarity of the Si surface from a negative dipole to a positive dipole, owing to the introduction of the SiO_x interface. The Si energy band will bend up and give rise to a favorable band alignment between Si and PEDOT:PSS to promote carrier separation. These results could be potentially employed to further development of this simple, low-cost heterojunction solar cell.

Keywords: SiO_x interface; n-Si/PEDOT:PSS solar cells; surface polarity

1. Introduction

Si/organic hybrid solar cells utilizing poly(3,4-ethylenedioxythiophene):poly(styrenesulfonate) (PEDOT:PSS) combined with an n-type silicon (n-Si) have attracted significant research interest in recent years due to their obvious advantages of a low-temperature process, remarkably low fabrication cost, and potential high efficiency [1]. In this type of hybrid solar cells, as shown in Figure 1, the PEDOT:PSS layer acts as a hole transporting path [2] when forming a heterojunction with the n-type Si substrate. Si has a strong absorption ability in a very wide spectrum range and excellent carrier transport ability. PEDOT:PSS is a water-soluble polymer which has a high conductivity, a transmission window in the visible spectral range, and excellent chemical and thermal stability. This type of Si/PEDOT:PSS hybrid solar cell combines the superior absorption property of Si in a wide spectrum range and the advantage of aqueous solution-based processes of PEDOT:PSS. Over the past few years, considerable progress towards creating highly efficient hybrid n-Si/PEDOT:PSS solar cells has been achieved by adjusting major factors such as electrical conductivity, chemical affinity, and passivation on the device surface [3–9]. Sun et al. introduced perovskite nanoparticles to the PEDOT:PSS layer to generate a positive electrical surface field [10]. Pham et al. presented adding functionalized graphene to the PEDOT:PSS solution based on Silicon nanowire (SiNW), and demonstrated an enhancement of photoelectric conversion efficiency (PCE). Wen et al. [11] fabricated an n+ amorphous silicon layer on

the back of the c-Si, which could significantly improve the extraction of the photon-generated carrier and suppress the recombination of hole electrons at the rear cathode [12]. Despite significant efforts to improve solar cell performance, the highest power conversion efficiency (PCE) reported to date is still low when compared to the value theoretically estimated by Shockley–Queisser for a single-junction device [13].

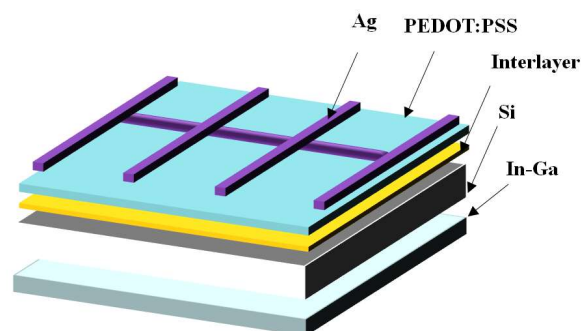


Figure 1. Schematic structure of planar hybrid n-Si/PEDOT:PSS solar cells.

To further improve the performance of the hybrid n-Si/PEDOT:PSS solar cells, the interface properties between n-Si and PEDOT:PSS are of great importance. This is because photogenerated holes in n-Si are required to be effectively transmitted through the heterojunction interface [1] into the PEDOT:PSS layer and then collected by the anode. Therefore, a high-quality interface between n-Si and PEDOT:PSS is critical for high-performance hybrid solar cells. However, usually, there are numerous microvoids at the Si/PEDOT:PSS interface because of the insufficient wettability of the Si surface, which leads to a bad surface coverage and severe recombination. A proper interface layer with a hydrophilic nature between the PEDOT:PSS and n-Si can improve the wettability of the Si surface, which is helpful in the formation of ideal interface contacts between the PEDOT:PSS film and the Si substrate, and thus a more ideal p–n junction, resulting in less charge recombination and a larger photocurrent density [14]. At the same time, the inserted interface layer may help to passivate the surface of n-Si, which could further enhance the device performance. As an effective interface layer between PEDOT:PSS and n-Si, its thickness is a critical parameter. When the interface layer is too thin, it is insufficient to provide good surface wettability and passivation. However, once the interface layer is too thick, the photogenerated carriers have difficulty when they tunnel through the insulating layer.

Previous work has shown improved solar cell performance when using a thin atomic layer deposition (ALD) Al_2O_3 layer [15,16], which was achieved based on increased built-in potential and improved charge collection by the electron blocking of Al_2O_3 . However, the ALD instrument is expensive, and the process is complex. Other oxide layers [17,18] are also reported to provide the crucial interface layer for the hybrid solar cells. However, all the reported deposition methods are complicated. As is well known, when Si is exposed to the air, a native oxide (SiO_x) will grow easily. As an efficient interface layer, its thickness is also important. We could remove the unintentionally grown oxide layer by dipping the Si substrate in a dilute HF solution and intentionally regrow the SiO_x layer by exposing the Si substrate to air in a simple and controllable way so that the wanted SiO_x thickness could be obtained. However, whether this oxide layer can effectively improve the interface quality and enhance the device performance or not is still not well investigated.

In this work, the effects of the SiO_x layer intentionally grown through exposure to air on the performance of planar hybrid n-Si/PEDOT:PSS solar cells are investigated. Compared to the cell with the bare Si surface, the cell with an oxygen-terminated Si surface reveals improved characteristics in power conversion efficiency (PCE), increased from 10.44% to 13.31%. It is inferred that the formation of oxygen-terminated bonds helps to build a net positive surface dipole, which promotes carrier separation and suppresses the Si surface recombination. Our results suggest promising strategies to further exploit the efficiency potential for the simple, low-cost hybrid Si/organic solar cells.

2. Results and Discussion

Figure 2 shows the oxide thickness (d_{ox}) of the Si substrates after exposure in air for different time periods. The thickness is measured by using the J. A. Woollam spectroscopic ellipsometer by fitting the ellipsometric data in the wavelength range of 300–1200 nm under an angle of incidence of 75° . When the substrate is immersed in the dilute HF solution, the native oxide is easily removed and the Si surface becomes the hydrogen-terminated (H-terminated) surface. The wettability of the H-terminated Si surface is poor, and it will lead to a bad surface coverage when the PEDOT:PSS is deposited later. Once the Si substrate is exposed in the air, the oxygen tends to react with the Si and form the SiO_x . After the Si substrate is taken out from the HF solution, we try to measure the SiO_x thickness as soon as possible. However, it is inevitable that the Si substrate will come into contact with the air, and this is why there is about 0.87 nm SiO_x for the sample with the 0 min exposure, as shown in Figure 2. For the first 60 min of the Si substrate exposure in the air, the SiO_x thickness increases nearly linearly as the time progresses (see the inset in Figure 2). After 360 min, the SiO_x thickness tends to saturate at about 3.1 nm. For better clarification in the following parts, we still name the sample with 0 min exposure in air as the H-terminated sample and other samples as the oxygen-terminated samples.

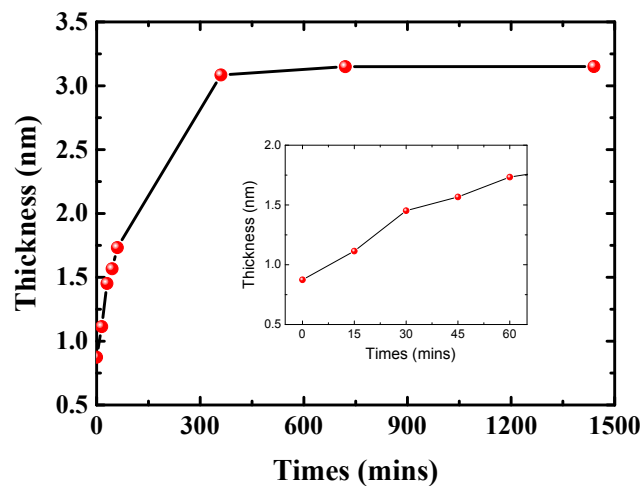


Figure 2. SiO_x thickness for the Si substrates exposed in air for different times.

Based on the formed SiO_x layer, the planar hybrid n-Si/PEDOT:PSS solar cells are fabricated, and Figure 3a shows the current density–voltage (J – V) characteristics of the devices under 100 mW/cm^2 illumination (AM(air mass) 1.5G), measured from a solar simulator. The J – V characteristics of photovoltaic (PV) cells can be approximately described by the Shockley equation:

$$J = J_0 \left(\exp \left(\frac{q(V - R_s J)}{nk_B T} \right) - 1 \right) + \frac{V - R_s J}{R_{sh}} - J_{ph} \quad (1)$$

where J_0 is the saturation current, J_{ph} the photo current, R_s the series resistance, R_{sh} the shunt resistance, n the ideality factor, q the electron charge, k_B the Boltzmann constant, and T the temperature. By using Equation (1) with our proposed explicit analytic expression method [19], the experimental data can be well rebuilt, as shown in Figure 3a, which confirmed the validity of the extracted parameters. By fitting the curves, the photovoltaic parameters of short-circuit current density (J_{sc}), open circuit voltage (V_{oc}), fill factor (FF), and PCE are extracted and summarized in Table 1. Figure 3b shows the variation of device parameters with different exposure times. For the H-terminated device, a PCE of 10.44% is achieved with a J_{sc} of 26.46 mA/cm^2 , a V_{oc} of 0.605 V, and an FF of 65.22%. For the device with 15 min exposure in air where the SiO_x thickness is 1.12 nm, all the device parameters of J_{sc} , V_{oc} , and FF are improved and the optimized device performance is achieved. The optimized device shows

a remarkable J_{sc} of 33.72 mA/cm^2 , V_{oc} of 0.607 V , and FF of 65.01% , which improves the overall PCE to 13.31% . For a much longer exposure time, the device performance begins to decrease. At 60 min exposure where the SiO_x thickness is 1.73 nm , the device only shows a J_{sc} of 26.45 mA/cm^2 , V_{oc} of 0.594 V , and FF of 59.58% , resulting in a PCE of 9.36% . It is guessed that the SiO_x can help enhance the uniformity of PEDOT:PSS, increase the built-in voltage (V_{bi}), and suppress recombination between the Si and PEDOT:PSS interface with a proper thickness, and thus improve the device performance. All the possible reasons will be discussed in the following part.

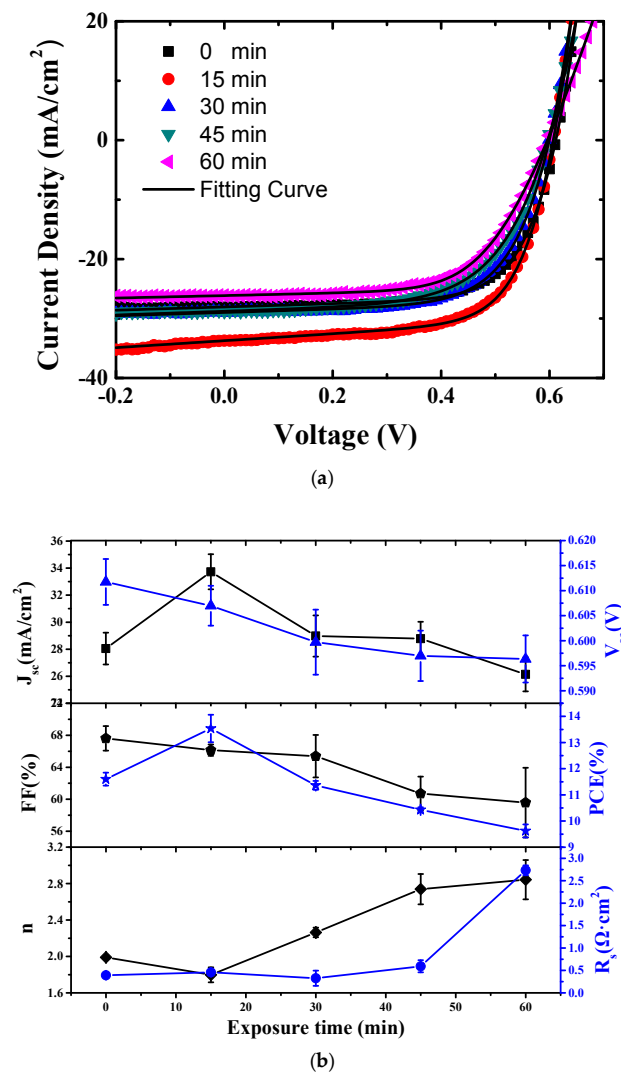


Figure 3. (a) J–V curves of the planar hybrid Si/PEDOT:PSS solar cells with different exposure times under 100 mW/cm^2 illumination (AM 1.5 G). (b) Variation of device parameters with different exposure times.

Table 1. Extracted parameters of the planar hybrid Si/PEDOT:PSS solar cells at a temperature of 27°C .

Time (min)	J_{sc} (mA/cm^2)	V_{oc} (V)	FF (%)	PCE (%)	n	R_s ($\Omega \cdot \text{cm}^2$)	R_{sh} ($\text{k}\Omega \cdot \text{cm}^2$)
0	26.46	0.605	65.22	10.44	1.99	3.9	0.37
15	33.72	0.607	65.01	13.31	1.79	4.5	0.17
30	28.97	0.599	64.42	11.19	2.26	3.2	0.36
45	28.784	0.596	60.17	10.33	2.74	5.9	0.32
60	26.45	0.594	59.58	9.36	2.8	27.3	0.48

In order to investigate the reason for the better performance of the optimized device, the capacitance–voltage (C – V) characteristics of the devices are measured by an Agilent 1500 A at a frequency of 1 MHz. Figure 4 shows the $1/C^2$ – V plot of the H-terminated and oxygen-terminated (15 min and 60 min) hybrid solar cells, and there is a linear relationship between $1/C^2$ and the applied voltage. The intercept of the line and the x -axis corresponds to V_{bi} [20]. All the devices show the same V_{bi} of around 0.8 V; this means that there is no difference of the built-in voltage for the different exposure times, which can be partially verified by observing almost the same V_{oc} around 0.60 V, as shown in Table 1. Since the different exposure times cannot change the V_{bi} , there should be other reasons for their different performances, which will be investigated in the following sections.

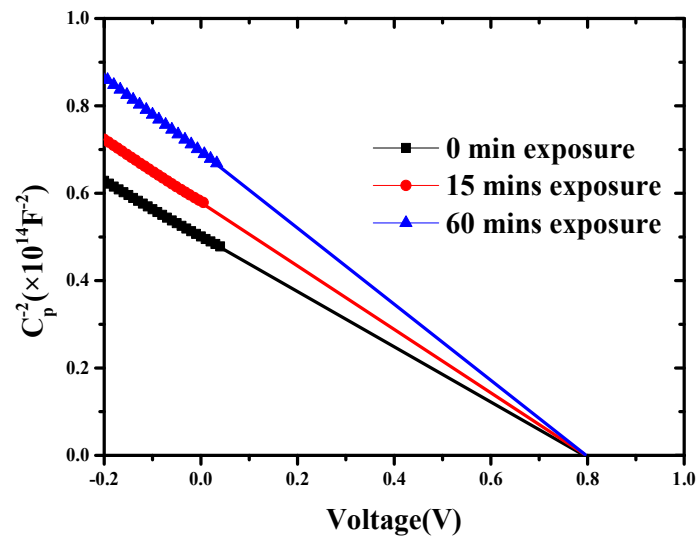


Figure 4. C – V measurements of the planar Si/PEDOT:PSS solar cells with different exposure times.

We measure the contact angles of PEDOT:PSS aqueous solution drops on the H-terminated and oxygen-terminated substrates to investigate the wettability of the samples. As shown in Figure 5, although the PEDOT:PSS solution is mixed with Triton X-100 as a surfactant to help the film formation, the fresh Si substrate (with 0 min exposure in air) still shows a large contact angle of 68.56° . With oxygen-terminated bonds instead of the H-terminated bonds, the contact angle begins to decrease, as indicated in Table 2. When the exposure time is 60 min, the contact angle is only 27.37° . This shows that a longer exposure time will produce thicker SiO_x , and then the more H-terminated bonds will be replaced by the oxygen-terminated bonds. Thus, the wettability of the Si surface is improved. The remarkably increased wettability of the Si surface after the exposure in air promotes easy spreading of the PEDOT:PSS solution, allowing for uniform covering of the surfaces. As a result, the number of surface defects in PEDOT:PSS, such as microvoids, which are easily formed during the spin-coating process and give rise to carrier recombination, are significantly reduced. Although a longer exposition time shows a better wettability, it should be noted that the main operation principle of our hybrid device is the tunneling of holes through the interface oxide layer. A thicker SiO_x normally prevents a tunneling process, and eventually holes are likely to be recombined with electrons. A thicker SiO_x leads to a high series resistance because of its electrically insulating nature, which induces a decreased FF, as shown in Table 1. This could partially explain why we could obtain the highest PCE with high values of J_{sc} and FF when the interlayer had a thickness of 1.12 nm, even though this sample does not show the best wettability. From this point of view, it seems that the wettability change may be one reason for their different performance.

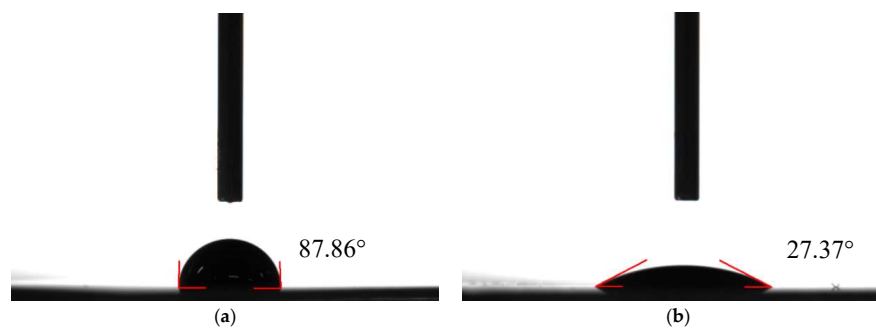


Figure 5. Contact angle images of PEDOT:PSS aqueous solution drops on the (a) H-terminated and (b) SiO_x-terminated silicon substrates.

Table 2. Contact angles of PEDOT:PSS drops on the H-terminated and oxygen-terminated silicon substrates.

Time (min)	0	15	30	45	60
θ (°)	87.86	68.56	48.51	39.80	27.37

Table 3. RMS values of the planar n-Si/PEDOT:PSS films with different exposure times.

Time (min)	0	15	30	45	60
RMS (nm)	2.64	2.57	2.57	2.55	2.29

The atomic force microscope (AFM) images of PEDOT:PSS layers coated on the Si substrates are shown in Figure 6. For all the films, the surfaces are relatively uniform with small root-mean-square (RMS) values between 2.29 nm and 2.64 nm, although the wettability of the samples are different, as shown in Table 3. The samples exposed in air for 15 min, 30 min, 45 min, and 60 min after being HF-etched only present slightly smaller RMS values than those of samples exposed in air for 0 min. Usually, the smooth surface would deliver fewer defects between the Si substrate and the PEDOT:PSS film to improve the efficiency of photogenerated carrier transportation. However, this should not be the main reason for the difference in device performance, since the differences of their RMS values are relatively small.

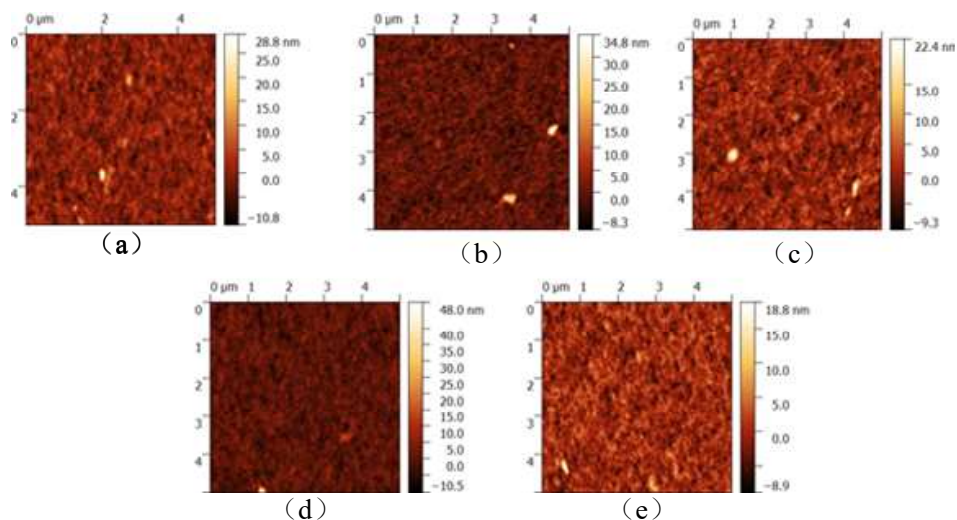


Figure 6. AFM images of PEDOT:PSS films with different exposure times of (a) 0 min; (b) 15 min; (c) 30 min; (d) 45 min; and (e) 60 min.

We also investigate the optical properties of n-Si/PEDOT:PSS structures by measuring the reflectance spectra. Figure 7 compares the reflectance of polished bare n-Si and n-Si/PEDOT:PSS samples with exposure to air for different time periods from 0 to 60 min. For all the samples, with the addition of the PEDOT:PSS film, the reflectance is greatly decreased, which shows that the PEDOT:PSS film has the function of being an antireflection layer. Compared to the samples with different exposure times, the reflectance is lowest for the H-terminated and oxygen-terminated (15 min) devices. The two samples show almost similar optical properties, and this means that the absorption difference is not the main reason for their difference in performance.

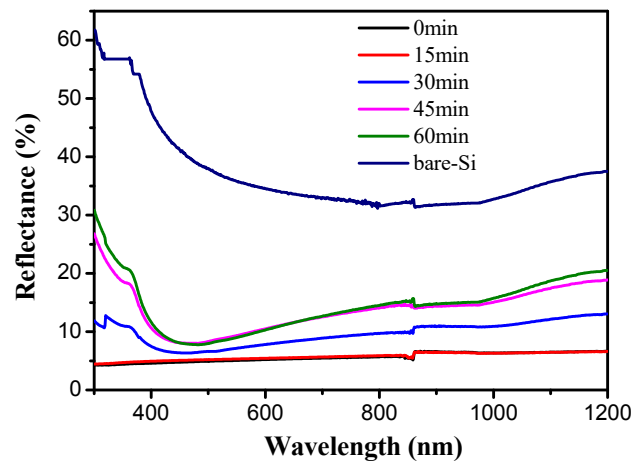


Figure 7. Reflection spectra of n-Si/PEDOT:PSS samples exposed to air for different time periods from 0 to 60 min; the reflection spectrum of the polished bare n-Si is also shown for a reference.

According to the above discussion, there are no obvious differences of V_{bi} , surface morphologies, and optical properties for the samples with different exposure times. The wettability change may be one reason for their different performance. However, the different wettability does not lead to the obviously different film morphologies of PEDOT:PSS, since the differences of their RMS values are relatively small. We believe that beyond the difference in wettability, there are other reasons for the different device performances. In order to interpret the performance differences for the H-terminated and oxygen-terminated (15 min) devices, the possible mechanism is proposed here. Figure 8a,b shows the energy band diagram of the H-Si/PEDOT:PSS and oxygen-Si/PEDOT:PSS heterojunctions, respectively. The electron affinity of bulk Si as shown is 4.05 eV [21]. Surface properties can either increase or decrease the effective electron affinity (χ_{eff}) at the Si surface relative to that in the bulk Si, depending on the polarity of the associated dipole [22]. It is reported that the H-Si surface would pose a net negative surface dipole upon the formation of the covalent H-Si surface bonds [21]. This leads to an increase in χ_{eff} at the Si/PEDOT:PSS surface and thus a bending down of the Si energy band near the Si/PEDOT:PSS interface, as shown in Figure 8a. As a result, a blocking internal electrical field exists and prevents the photoexcited holes in the Si from injecting into PEDOT:PSS, resulting in higher carrier recombination at the interface. However, the oxygen-terminated Si surface is reported to pose a net positive surface dipole, and this will lead to the drop of χ_{eff} . Accordingly, the Si energy band will bend up and give rise to a favorable band alignment between oxygen-Si and PEDOT:PSS to promote carrier separation. Moreover, the SiO_x layer can passivate the Si surface and help in suppressing the Si surface recombination. This could be partially verified by the increased J_{sc} , as shown in Figure 3. However, a thicker SiO_x layer would become a barrier for charge transport in the cells, leading to a higher series resistance. This is why there is an optimized SiO_x thickness.

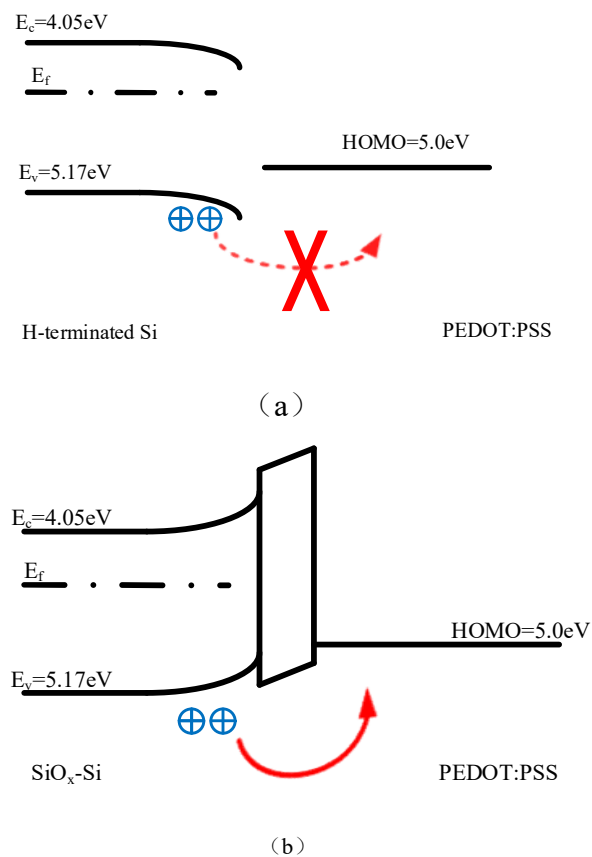


Figure 8. The energy band diagram of the (a) H-Si/PEDOT:PSS and (b) SiO_x-Si/PEDOT:PSS hybrid heterojunctions.

3. Materials and Methods

3.1. Film Formation and Device Fabrication

The devices were fabricated according to the sequences below: The n-type (100) single-sided polished silicon wafers (resistivity: 0.05–0.1 Ω -cm) with thickness of 300 ± 10 μm were cut into 15×15 mm squares as the substrates. The Si substrates were ultrasonically cleaned in acetone, alcohol, and ionized water sequentially for 15 min. The native oxide on the substrates were etched by immersing the Si substrates in a dilute HF (5%) solution for 30 s and dried by N₂ for later use. After the removal of the native oxide layer, there were H-terminated bonds on the Si surface. A highly conductive PEDOT:PSS solution (PH1000, Heraeus Clevios) was filtered with a polyvinylidene fluoride membrane (0.45 μm porosity) to remove agglomerations. 7% ethylene glycol and 1% Triton X-100 were added to the PEDOT:PSS solution to improve the wettability and conductivity. All the Si substrates were divided into five groups and exposed to air for the different time periods of 0 min, 15 min, 30 min, 45 min, or 60 min, respectively. The PEDOT:PSS solution was then spin-coated on the H-terminated (0 min) and SiO_x-terminated (exposed to air for 15 min, 30 min, 45 min, or 60 min, respectively) substrates at a speed of 2500 rpm for 60 s. After the PEDOT:PSS deposition, the samples were annealed on a hot plate at 190 $^{\circ}\text{C}$ for 15 min to remove the solvent to form a uniform and conductive p-type organic thin film. A 150-nm thick Ag film was thermally evaporated to form a grid as the front contact. Finally, the eutectic In–Ga alloy was used to fully cover the rear side of the Si substrate to form an ohmic contact.

3.2. Device Characterization

The morphology measurements of the PEDOT:PSS films were measured by atomic force microscopy (AFM, Agilent 5500). The UV–visible reflection spectra were recorded with a UV–visible reflection spectrophotometer (Perkin-Elmer Lambda 950). The thickness of the SiO_x layer was measured by spectroscopic ellipsometry (Jawoolam M-2000). Photovoltaic parameters were measured using a Keithley 2400 source meter under simulated sunlight from a XES-70S1 solar simulator matching the AM 1.5G standard with an intensity of 100 mW/cm². The system was calibrated against a National Renewable Energy Laboratory (NREL)-certified reference solar cell. The capacitance–voltage characteristics were measured by an Agilent 1400 semiconductor parameter analyzer. All the measurements of the solar cells were performed under an ambient atmosphere at room temperature without any encapsulation.

4. Conclusions

In summary, we demonstrated that the exposure-oxidation treatment of an H-terminated Si substrate could enhance the performance of planar hybrid Si/PEDOT:PSS solar cells. After the oxidation, the Si surface wettability could be improved, which is ascribed to the hydrophilicity of the SiO_x layer, allowing an effective spread of the PEDOT:PSS and thus a good contact between the PEDOT:PSS film and Si. More importantly, it can change the polarity of the Si surface from a negative dipole to a positive dipole, owing to the formation of covalent oxygen–Si bonds. The Si energy band bends up and gives rise to a favorable band alignment between oxygen-terminated Si and PEDOT:PSS to promote carrier separation. These results could be potentially employed to further the development of this simple, low-cost heterojunction solar cell.

Author Contributions: C.Z. (Chunfu Zhang) and Y.Z. conceived the idea and guided the experiment; C.Z. (Chenxu Zhang) conducted most of the device fabrication and data collection; C.Z. (Chunfu Zhang) revised the manuscript; H.G., Q.J., and P.D. helped with the device measurements. All authors read and approved the manuscript.

Acknowledgments: We thank the Natural Science Foundation of China (61604119), Fundamental Research Funds for the Central Universities (Grant No. JBX171103, JB161101, JB161102), Class General Financial Grant from the China Postdoctoral Science Foundation (Grant No. 2016M602771), the Funds for University from Department of Education of Guangxi (KY2015YB109), and the Funds for the Key Laboratory of Automatic Measurement Technology and Instruments (YQ16103).

Conflicts of Interest: The authors declare no conflict of interest.

References

1. Pietsch, M.; Bashouti, M.Y.; Christiansen, S. The role of hole transport in hybrid inorganic/organic silicon/poly(3,4-ethylenedioxy-thiophene):poly(styrenesulfonate) heterojunction solar cells. *J. Phys. Chem. C* **2013**, *117*, 9049–9055. [[CrossRef](#)]
2. Jäckle, S.; Mattiza, M.; Liebhaber, M.; Brönstrup, G.; Rommel, M.; Lips, K.; Christiansen, S. Junction formation and current transport mechanisms in hybrid n-Si/PEDOT:PSS solar cells. *Sci. Rep.* **2015**, *5*, 13008. [[CrossRef](#)] [[PubMed](#)]
3. Ouyang, J.; Xu, Q.; Chu, C.W.; Yang, Y.; Li, G.; Shinar, J. On the mechanism of conductivity enhancement in poly(3,4-ethylenedioxythiophene):poly(styrene sulfonate) film through solvent treatment. *Polymer* **2004**, *45*, 8443–8450. [[CrossRef](#)]
4. Liu, Q.; Ono, M.; Tang, Z.; Ishikawa, R.; Ueno, K.; Shirai, H. Highly efficient crystalline silicon/Zonyl fluorosurfactant-treated organic heterojunction solar cells. *Appl. Phys. Lett.* **2012**, *100*, 183901. [[CrossRef](#)]
5. Zhang, Y.; Liu, R.; Lee, S.T.; Sun, B. The role of a LiF layer on the performance of poly(3,4-ethylenedioxythiophene):poly(styrenesulfonate)/Si organic-inorganic hybrid solar cells. *Appl. Phys. Lett.* **2014**, *104*, 083514. [[CrossRef](#)]
6. Zhang, Y.; Zu, F.; Lee, S.T.; Liao, L.; Zhao, N.; Sun, B. Heterojunction with organic thin layers on silicon for record efficiency hybrid solar cells. *Adv. Energy Mater.* **2014**, *4*. [[CrossRef](#)]

7. Xia, Z.; Song, T.; Sun, J.; Lee, S.T.; Sun, B. Plasmonic enhancement in hybrid organic/Si heterojunction solar cells enabled by embedded gold nanoparticles. *Appl. Phys. Lett.* **2014**, *105*, 241110. [[CrossRef](#)]
8. Schaadt, D.M.; Feng, B.; Yu, E.T. Enhanced semiconductor optical absorption via surface plasmon excitation in metal nanoparticles. *Appl. Phys. Lett.* **2005**, *86*, 063106. [[CrossRef](#)]
9. Shen, X.; Xia, Z.; Chen, L.; Li, S.; Zhao, J. Optical and electrical enhancement for high performance hybrid Si/organic heterojunction solar cells using gold nanoparticles. *Electrochim. Acta* **2016**, *222*, 1387–1392. [[CrossRef](#)]
10. Wang, Y.; Xia, Z.; Liu, L.; Xu, W.; Yuan, Z.; Zhang, Y.; Siringhaus, H.; Lifshitz, Y.; Lee, S.; Sun, B. The Light Induced Field Effect Solar Cell Concept Perovskite Nanoparticle Coating Introduces Polarization Enhancing Silicon Cell Efficiency. *Adv. Mater.* **2017**, *29*. [[CrossRef](#)] [[PubMed](#)]
11. Van Trinh, P.; Hong, P.N.; Thang, B.H.; Hong, N.T.; Thiet, D.V.; Chuc, N.V.; minh, P.N. Effect of Surface Morphology and Dispersion Media on the Properties of PEDOT:PSS/n-Si Hybrid Solar Cell Containing Functionalized Graphene. *Adv. Mater. Sci. Eng.* **2017**, *2017*, 2362056. [[CrossRef](#)]
12. Wen, H.; Cai, H.; Du, Y.; Dai, X.; Sun, Y.; Ni, J.; Li, J.; Zhang, D.; Zhang, J. Improving the organic/Si heterojunction hybrid solar cell property by optimizing PEDOT: PSS film and with amorphous silicon as back surface field. *Appl. Phys. A* **2017**, *123*, 14. [[CrossRef](#)]
13. Chen, T.G.; Huang, B.Y.; Chen, E.C.; Yu, P.; Meng, H.F. Micro-textured conductive polymer/silicon heterojunction photovoltaic devices with high efficiency. *Appl. Phys. Lett.* **2012**, *101*, 033301. [[CrossRef](#)]
14. He, L.; Jiang, C.; Wang, H.; Lai, D.; Rusli. High efficiency planar Si/organic heterojunction hybrid solar cells. *Appl. Phys. Lett.* **2012**, *100*, 073503. [[CrossRef](#)]
15. Junghanns, M.; Plentz, J.; Andrä, G.; Gawlik, A.; Höger, I.; Falk, F. PEDOT:PSS emitters on multicrystalline silicon thin-film absorbers for hybrid solar cells. *Appl. Phys. Lett.* **2015**, *106*, 083904. [[CrossRef](#)]
16. Nam, Y.H.; Song, J.W.; Park, M.J.; Sami, A.; Lee, J.H. Ultrathin Al₂O₃ interface achieving an 11.46% efficiency in planar n-Si/PEDOT:PSS hybrid solar cells. *Nanotechnology* **2017**, *28*, 155402. [[CrossRef](#)] [[PubMed](#)]
17. Liu, Y.; Zhang, J.; Wu, H.; Cui, W.; Wang, R.; Ding, K.; Sun, B. Low-temperature synthesis TiO_x, passivation layer for organic-silicon heterojunction solar cell with a high open-circuit voltage. *Nano Energy* **2017**, *34*, 257–263. [[CrossRef](#)]
18. Sheng, J.; Fan, K.; Wang, D.; Han, C.; Fang, J.; Gao, P.; Ye, J. Improvement of the SiO_x passivation layer for high-efficiency Si/PEDOT:PSS heterojunction solar cells. *ACS Appl. Mater. Interfaces* **2014**, *6*, 16027–16034. [[CrossRef](#)] [[PubMed](#)]
19. Zhang, C.; Zhang, J.; Hao, Y.; Lin, Z.; Zhu, C. A simple and efficient solar cell parameter extraction method from a single current-voltage curve. *J. Appl. Phys.* **2011**, *110*, 064504. [[CrossRef](#)]
20. Zhang, J.; Zhang, Y.; Zhang, F.; Sun, B. Electrical characterization of inorganic-organic hybrid photovoltaic devices based on silicon-poly(3,4-ethylenedioxythiophene):poly(styrenesulfonate). *Appl. Phys. Lett.* **2013**, *102*, 013501. [[CrossRef](#)]
21. Hunger, R.; Fritsche, R.; Jaeckel, B.; Jaegermann, W.; Webb, L.J.; Lewis, N.S. Chemical and electronic characterization of methyl-terminated Si(111) surfaces by high-resolution synchrotron photoelectron spectroscopy. *Phys. Rev. B Condens. Matter* **2005**, *72*, 045317. [[CrossRef](#)]
22. Maldonado, S.; Plass, K.E.; Knapp, D.; Lewis, N.S. Electrical Properties of Junctions between Hg and Si(111) Surfaces Functionalized with Short-Chain Alkyls. *J. Phys. Chem. C* **2007**, *111*, 17690–17699. [[CrossRef](#)]

